Computer & Robotics

Adaptive Sliding Mode Tracking Control of Mobile Robot in Dynamic Environment Using Artificial Potential Fields

Abolfath Nikranjbar [a,*], Masoud Haidari [a], Ali Asghar Atai [b]

[a] *Mechanical Engineering Department, Islamic Azad University, Karaj Branch, Iran*
[b] *School of Mechanical Engineering, College of Engineering, University of Tehran, Iran*

Received 28 June 2017; revised 8 August 2017; accepted 30 November 2017; available online 15 March 2018

Abstract

Solution to the safe and collision-free trajectory of the wheeled mobile robot in cluttered environments containing the static and/or dynamic obstacle has become a very popular and challenging research topic in the last decade. Notwithstanding of the amount of publications dealing with the different aspects of this field, the ongoing efforts to address the more effective and creative methods is continued. In this article, the effectiveness of the real-time harmonic potential field theory based on the panel method to generate the reference path and the orientation of the trajectory tracking control of the three-wheel nonholonomic robot in the presence of variable-size dynamic obstacle is investigated. The hybrid control strategy based on a backstepping kinematic and regressor-based adaptive integral sliding mode dynamic control in the presence of disturbance in the torque level and parameter uncertainties is employed. In order to illustrate the performance of the proposed adaptive algorithm, a hybrid conventional integral sliding mode dynamic control has been established. The employed control methods ensure the stability of the controlled system according to Lyapunov's stability law. The results of simulation program show the remarkable performance of the both methods as the robust dynamic control of the mobile robot in tracking the reference path in unstructured environment containing variable-size dynamic obstacle with outstanding disturbance suppression characteristic.

Keywords: *Adaptive Control, Sliding Mode, Perturbation Estimation, Trajectory Tracking, Rigid Robot Manipulators.*

1. Introduction

Wheeled Mobile Robots (WMRs) are the most widely used among the class of Mobile Robots. This is due to their fast manoeuvring, simple control and energy saving characteristics [1]. These devices are becoming increasingly important in industry as a means of transport, inspection, and operation because of their efficiency and flexibility. In addition, mobile robots are useful for intervention in hostile environments performing tasks such as handling solid radioactive waste, decontaminating nuclear reactors, handling filters, patrolling buildings, minesweeping, etc. Furthermore, mobile robots can serve as a test platform for a variety of experiments in sensing the environment and making intelligent choices in response to it [2]. In all above applications, the robot may be faced with

* Corresponding author. Email: a.nikranjbar@kiau.ac.ir

different static or dynamic obstacles that should be able to safely avoid them.

The mobile robot in obstacle avoidance is faced with two issues that must be considered simultaneously. First, designing the reference trajectory (from start to target point) generating algorithm in presence of static/dynamic obstacle [3], and second, designing the controller for tracking this reference trajectory. However, in most researches, the simultaneous study of these two issues has not been carried out appropriately [4-6].

One of the widely used algorithms in trajectory generation for the robotic applications is the artificial potential field (APF) method. The first use of APF in trajectory generation for mobile robots dates back to 1986 [7]. The benefits of this approach gained much attention in the field of WMRs. The local minimum, which is the basic problem with methods based on potential fields, was eliminated by the introduction of harmonic potential functions having spherical symmetry [8]. Another issue was representing the geometry of the obstacle in a simple way. Some authors used circles enclosing the obstacle, which proved to be inefficient for the case of long and narrow shapes, with the chance of embracing the starting point or the goal [4, 9]. To overcome this problem, the panel method was introduced for better representing the irregular shaped obstacles, in which each panel is a line of distributed source/sinks [8]. The salient feature in the panel method was to select velocities of particles at the centre of each panel in such a way that the total obstacle repulsive strength becomes less than the goal's attractive strength, so that the robot does not miss the goal. The value of these velocities is highly dependent on the geometry of obstacles, and cannot be found through trial and error. An elegant method, which automatically adjusts these velocities so that the above-mentioned constraint is satisfied, was proposed by Fahimi et al., first in the form of research articles [10,11], and then with more detail in his book [12] , followed by research article [13] . The specific feature of the harmonic potential functions not suffering from the local minima and leading to the unique solution [12], specially associated with the panel method, gained remarkable attention among the researchers. Since then, several authors have used this approach in the field of mobile robots and manipulators [14-19]. In more recent publication, generating potential field using Laplace equation along with Dirichlets conditions is addressed in [19]. Finite difference approximation method is used to find the numerical solution of Laplace equation. It is shown the smooth generated streamlines enables the robot to completely avoid the obstacles. However, the solution is limited to the geometrically not complicated arrangements while considering the kinematics of the robot.

Nonholonomic mobile robots have limitations imposed on their velocity which cannot be integrated to be transformed to position constraints [20]. Consequently controlling the position of these types of robots is more challenging and hence an important class of control problem [20]. Much has been written about motion control under nonholonomic constraints using the kinematic model of the mobile robot [21]. In practice, this kinematics cannot be achieved without considering the system's dynamics. This has motivated researchers to address the integration of nonholonomic kinematic controller along with the control of the dynamic of the mobile robot [17, 21-23].

Due to highly nonlinear nature of the kinematics and dynamics of the mobile robot, nonlinear control approaches have been adopted by most researchers [17, 20-22, 24]. One of the appropriate methods for the kinematic control of this class of robots is the backstepping method, which was developed in early 1990s for a class of expanded nonlinear dynamic systems [25]. In this recursive structure, the system is decomposed into subsystems that cannot be simplified and the stability of each subsystem is established using methods such as Lyapunov Stability Theory. Once the stability of the subsystems are ensured through a step-by-step recursive algorithm to outer system, a controller is designed and then the stability of the whole system is assured [25, 26].

Due to the effectiveness of the cited control algorithm, specifically direct applicability for controlling nonlinear systems, it has found great usage in WMR applications. A combined kinematic/torque control law using backstepping control algorithm was applied to the three basic nonholonomic navigation problems (tracking a reference trajectory, path following, and stabilization about a desired posture [21].

Sliding mode control is a well-known nonlinear control method which is insensitive to variations of the plant parameters and uncertainties and acts as a complete elimination of unexpected input disturbances, while maintaining the stability of the controlled system [27].

As an example of usage of this algorithm in control of WMRs, a second-order sliding-mode controller was designed and was capable of making a three -wheeled vehicle follow a trajectory generated by an original gradient-based mechanism and its robustness was shown in comparison to first-order sliding-mode controller [9, 17]. The effectiveness of the proposed controller in tracking the reference path generated by artificial potential field method was compared to the controller given in [21, 22] while the robot was subjected to the disturbance torques acting on the wheels. In another application, the exponential sliding mode control proposed for trajectory tracking of nonholonomic WMRs, presenting a new solution to the problem of chattering in variable structure control [28]. The last but not the least, the performance of the PID based sliding mode control combined with the fuzzy controller to reduce the chattering phenomena in controlling the WMR, was compared with the feedback linearization and the pure sliding mode controllers [29].

A common point with these research publications to be addressed is that the bounds of the disturbances and parameter uncertainties are presumed to be known. This issue evidently limits the results to the applications with the known and prespecified parameters and uncertainties. To overcome this problem, a generalized adaptive sliding mode control is considered by researchers.

The performance of the combined back-stepping kinematic and PI adaptive sliding mode dynamic control based on the adaptation of the gains of the switching part of the controller of the nonholonomic mobile robot susceptible to parameter uncertainties and input disturbances was compared to conventional sliding mode method. The real test revealed the manoeuvrability of the robot according to the proposed algorithm [22]. Another publication investigating the performance of the regressor-based sliding mode control effort along with the matrix of the dynamic model uncertainties showed the acceptable performance of the algorithm, despite the significant range of variation of the plant parameters [30].

In this research, a combined hybrid backstepping kinematic control along with the regressor based adaptive integral sliding mode kinetic control of the three-wheeled nonholonomic mobile robot susceptible to parameter uncertainties and input disturbances is investigated. The proposed control method benefits the real-time panel method potential field algorithm for developing the robot trajectory in unstructured environment containing variable-size dynamic obstacle. The effectiveness of the proposed controller in tracking the reference path generated using real-time artificial potential field method is compared to the controller given in [16] while the robot is subjected to the disturbance torques acting on the wheels of robot.

2. Nonholonomic Mobile Robot

The general schema of a nonholonomic WMR is shown in Fig. 1. It consists of two standard fixed wheels with lateral slide constraint and one spherical omnidirectional or castor wheel to maintain the WMR's stability, which does not impose any limitations on the kinematics of the robot body [3]. Independent actuators, providing the necessary torques to drive the wheels, achieve the motion and orientation. The moving coordinate system fixed on the robot is considered with the origin at point P, located in the middle of the main driving wheels, and with xc oriented along the longitudinal direction of the robot. In addition, the centroid of the WMR is located at point G having a distance d from the axis of driving wheels. The position and orientation of the robot measured in inertial frame {xoy} is specified by the vector $\mathbf{q} = \left[x,\ y,\ \theta\right]^T$.

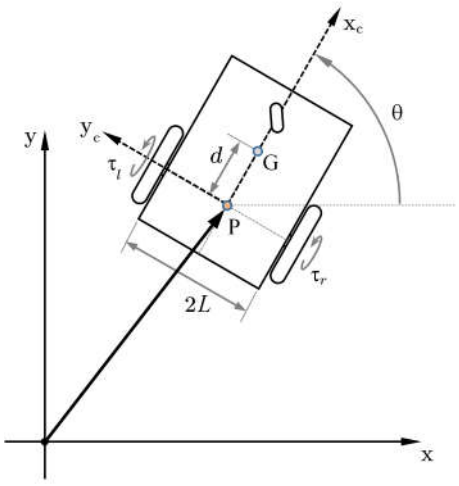

Fig. 1. A simple model of a three – wheel nonholonomic mobile robot

The lateral no slip condition of the driving wheels limits the movement of the robot at any instance only in the direction perpendicular to the axes of the driving wheels. This results in the following nonholonomic constraint [31]:

$$\dot{y}\cos\theta - \dot{x}\sin\theta = 0 \quad (1)$$

Considering Eq. 1, the kinematic model of wheeled mobile robots at point P can be expressed as follows:

$$\dot{\mathbf{q}} = \begin{bmatrix} \dot{x} \\ \dot{y} \\ \dot{\theta} \end{bmatrix} = \begin{bmatrix} \cos\theta & 0 \\ \sin\theta & 0 \\ 0 & 1 \end{bmatrix} \begin{bmatrix} v(t) \\ \omega(t) \end{bmatrix} = \mathbf{S}(\mathbf{q})\mathbf{v}(t) \quad (2)$$

Where v and ω are the linear and angular speed of the point P of the robot, respectively. Eq. 2 is the so-called guiding system of wheeled mobile robots, in which $\mathbf{S(q)}$ a Jacobian matrix that transforms $\mathbf{v}$ (the speed vector in the moving coordinates) to $\dot{\mathbf{q}}$ (the speed vector in the inertial reference Cartesian coordinates).

According to [21, 22], the well-known dynamic equation of the mobile robot system with n-generalized coordinates $\mathbf{q} \in R^{n\times 1}$, and $r(=n-k)$ inputs (m being the no. of constraints), can be described as

$$\mathbf{M}(\mathbf{q})\ddot{\mathbf{q}} + \mathbf{C}(\mathbf{q},\dot{\mathbf{q}})\dot{\mathbf{q}} + \boldsymbol{\tau}_d = \mathbf{B}(\mathbf{q})\boldsymbol{\tau} - \mathbf{A}(\mathbf{q})\boldsymbol{\lambda} \quad (3)$$

Where $\mathbf{M}(\mathbf{q}) \in R^{n\times n}$ is the symmetric positive definite inertia matrix, $\mathbf{C}(\mathbf{q},\dot{\mathbf{q}}) \in R^{n\times n}$ is the Centripetal and Coriolis matrix. $\boldsymbol{\tau}_d \in R^{n\times 1}$ denotes bounded unknown disturbances including unstructured unmodeled dynamics, $\mathbf{B}(\mathbf{q}) \in R^{n\times r}$ is the input transformation matrix, $\boldsymbol{\tau} \in \mathrm{R}^{r\times 1}$ is a control input vector, $\mathbf{A}(\mathbf{q}) \in R^{n\times k}$ is a matrix associated with the nonholonomic constraints, $\boldsymbol{\lambda} \in R^{k\times 1}$ is the Lagrange multiplier associated with the constraints, $\dot{\mathbf{q}}$ and $\ddot{\mathbf{q}}$ denote generalized velocity and acceleration vectors, respectively.

These variables in expanded form are given by

$$\mathbf{M} = \begin{bmatrix} m & 0 & -md\sin\theta \\ 0 & m & md\cos\theta \\ -md\sin\theta & md\cos\theta & I_G + md^2 \end{bmatrix}$$

$$\boldsymbol{\tau} = \begin{bmatrix} \tau_l \\ \tau_r \end{bmatrix}, \mathbf{C} = \begin{bmatrix} 0 & 0 & -md\dot{\theta}\cos\theta \\ 0 & 0 & -md\dot{\theta}\sin\theta \\ 0 & 0 & 0 \end{bmatrix}$$

$$\mathbf{B} = \frac{1}{r}\begin{bmatrix} \cos\theta & \cos\theta \\ \sin\theta & \sin\theta \\ -L & L \end{bmatrix}, \mathbf{A} = \begin{bmatrix} -\sin\theta \\ \cos\theta \\ 0 \end{bmatrix}$$

Where m and I_G are the mass and inertia about the centre of gravity of the robot, respectively. L Is the distance from the active wheel to the centre of the robot chassis? d Is the distance of the centre of gravity of the robot to the origin of the moving coordinate along the x_c axis; r is the radius of the active wheels of the robot; τ_l and τ_r are torques acting on the left and right active wheels, respectively.

The Dynamic equation (3) along with the constraint equation (2) fully describe the kinematics of the robot system. However, the Lagrange multiplier $\boldsymbol{\lambda}$ in (3) cannot be measured and controlled by the control system. The concept of null space is utilized to eliminate the Lagrange multiplier in the equations [31]. The null space $\mathbf{S(q)}$ of $\mathbf{A(q)}$ are determined by solving the inner production equation

$$\mathbf{A}^T(\mathbf{q})\mathbf{S}(\mathbf{q}) = 0 \quad (4)$$

In brief, by left-multiplying (3) by $\mathbf{S}^T$, making use of (4) to eliminate $\boldsymbol{\lambda}$, and substituting for $\dot{\mathbf{q}}$ and $\ddot{\mathbf{q}}$ from (2), eq. 3 is transformed to the following form [31].

$$\bar{\mathbf{M}}\dot{\mathbf{v}} + \bar{\mathbf{V}}\mathbf{v} + \boldsymbol{\delta}_{\tau} = \bar{\mathbf{B}}\boldsymbol{\tau} \quad (5)$$

Where $\bar{\mathbf{M}} = \mathbf{S}^{\mathrm{T}}\mathbf{M}\mathbf{S} \in R^{2\times 2}$, $\bar{\mathbf{V}} = \mathbf{S}^{\mathrm{T}}(\mathbf{M}\dot{\mathbf{S}} + \mathbf{V}\mathbf{S}) \in R^{2\times 2}$, $\bar{\mathbf{B}} = \mathbf{S}^{\mathrm{T}}\mathbf{B} \in R^{2\times 2}$ and $\boldsymbol{\delta}_{\tau} \in R^{2\times 1}$ are the transformed mass, nonlinearities, input torque matrices and the external disturbance vector, respectively, and are expressed in expanded form as

$$\bar{\mathbf{M}} = \begin{bmatrix} m & 0 \\ 0 & I_G + md^2 \end{bmatrix}, \bar{\mathbf{V}} = \begin{bmatrix} 0 & -md\dot{\theta} \\ md\dot{\theta} & 0 \end{bmatrix}$$

$$\bar{\mathbf{B}} = \frac{1}{r}\begin{bmatrix} 1 & 1 \\ -L & L \end{bmatrix}, \boldsymbol{\delta}_{\tau} = \begin{bmatrix} \delta_{\tau_l} \\ \delta_{\tau_r} \end{bmatrix}$$

In which δ_{τ_l} and δ_{τ_r} are the left and right components of the external disturbance vector, respectively. It should be noted that, $\bar{\mathbf{M}}$ and $\bar{\mathbf{V}}$ could involve uncertainties.

Once the vector $\mathbf{v}$ is obtained by solving eq. 4, then eq. 2 is employed to transform the state variables to the rate of the generalized coordinates $\dot{\mathbf{q}}$, which is then used to calculate the generalized state coordinates $\mathbf{q}$.

3. Harmonic Potential Field Path Planning

In the artificial potential field method, an attracting potential is used for the target position and repelling potentials are employed for the obstacles in the area where the robot operates. To deal with the issue of trapping in local minimums (a common problem in potential field models), the harmonic potential fields are used. Under proper conditions [32], this method causes the total elimination of local minimums. The harmonic functions used in this method follow Laplace's equation:

$$\nabla^2\phi = 0 \tag{6}$$

Two groups of potential functions are required in the formation of artificial potential fields: the first group guides mobile robots to the desired (goal) position and the second prevents robots from running into obstacles. The use of an attractive potential sink at the target position, and the employment of a reinforcing effect in the form of a uniform potential flow that connects the starting point to the target (goal) point, are useful in guiding the robot to the desired position. These functions comprising the first group, are defined as follows [12]:

$$\phi_g = \frac{\lambda_g}{4\pi}\ln(R_g) \tag{7}$$

$$\phi_u = -U\left(x\cos\alpha + y\sin\alpha\right) \tag{8}$$

In above equations, $R_g = (x-x_g)^2 + (y-y_g)^2$ in which (x_g, y_g) are the coordinates of the target, λ_g is the power of the target sink, U is the strength of the uniform flow, and α is the angle between the x axis and the direction of the uniform flow.

The second group consist of functions developed on the panel method, in which the boundaries of the obstacle in two dimensions are approximated by m line segments called panels [12]. Each panel j is modelled as a uniformly distributed source with strength per unit length λ_j along the panel. The potential function of each panel is defined as follows:

$$\phi_{oj} = \frac{\lambda_j}{4\pi}\int_j \ln R_j dl_j \tag{9}$$

In equation (9), $R_j = (x-x_j)^2 + (y-y_j)^2$ in which (x_j, y_j) is an arbitrary point on the j^{th} panel.

Employing the principle of superposition, the total artificial potential at any point in the field is obtained by summation of the individual harmonic potential functions.

$$\begin{aligned}\phi_{total} &= \phi_u + \phi_g + \sum_{j=1}^{m}\phi_{oj} \\ &= -U\left(x\cos\alpha + y\sin\alpha\right) \\ &\quad + \frac{\lambda_g}{4\pi}\ln R_g \\ &\quad + \sum_{j=1}^{m}\frac{\lambda_j}{4\pi}\int_j \ln R_j dl_j\end{aligned} \tag{10}$$

In Fig. 2, the concept of the artificial potential field in the presence of an unstructured obstacle is depicted.

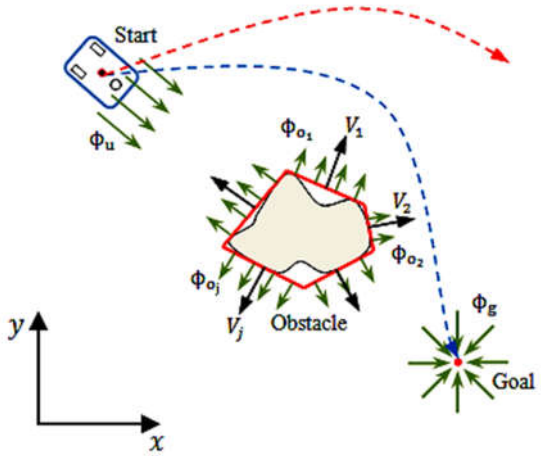

Fig. 2. An artificial potential field in the presence of an obstacle

In WMR control applications, the strength of the uniform flow U and the strength of the goal sink λ_g are usually specified. Then, at least m independent equations are needed to solve the problem in order to calculate the strength of the m panels. If the outward normal velocities generated at the centre $[(x_{ci}, y_{ci}), i = 1, \ldots, m]$ of the m panels are specified, these m equations can be derived as [12].

$$\frac{\partial}{\partial n_i}\phi\left(x_{ci}, y_{ci}\right) = -V_i, \quad i = 1,\ldots,m \tag{11}$$

It is noted that m normal outward speed of $V_i (> 0, i = 1, \cdots, m)$ must be selected such that the following conditions are satisfied:

$$-\lambda_g > \lambda_o \left(= \sum_{j=1}^{m}\lambda_j L_j\right) > 0 \tag{12}$$

Where λ_o represents the total repellent power of the panels.

Eq. (12) emphasizes on the condition that the potential function of (10) has only one global minimum at the location of the goal sink.

The convergence condition (12) indicates that the summation of obstacle repulsive strengths is less than the goal attractive strength, and its satisfaction guarantees that the goal is the global minimum of the potential and the robot does not miss it [12]. The value of these velocities highly depend on the size and shape of the obstacles. Since the sizes of the obstacles are different for different path planning problems, it is impossible to decide the value of normal velocities by trial and error. Therefore, a method for automatically adjusting the potential field parameters based on the obstacle sizes is evidently necessary.

The velocity components of the corresponding artificial potential field at any point of the operational space of robot using the relationship $\mathbf{v} = [\mathrm{u}, \mathrm{v}]^T = -\nabla\phi$ along with the equation (10) are obtained as:

$$\begin{aligned} u &= U\cos\alpha - \frac{\lambda_g}{4\pi}\frac{\partial}{\partial x}\ln R_g \\ &\quad -\sum_{j=1}^{m}\frac{\lambda_j}{4\pi}\int_j \frac{\partial}{\partial x}\ln R_j dl_j \\ v &= U\sin\alpha - \frac{\lambda_g}{4\pi}\frac{\partial}{\partial y}\ln R_g \\ &\quad -\sum_{j=1}^{m}\frac{\lambda_j}{4\pi}\int_j \frac{\partial}{\partial y}\ln R_j dl_j \end{aligned} \tag{13}$$

The direction of the speed vector throughout the field is calculated as:

$$\theta = \arctan\left(\frac{v}{u}\right) \tag{14}$$

The resultant speed vector $\mathbf{v}$ provides the information to build up the robot-desired path connecting the start-up point to the target. A desired speed of robot could be achieved along the path by changing the magnitude of the speed at any point while maintaining the orientation of the WMR using potential field data.

The algorithm can be extended to the real time applications, as the robot has to be safely interact with the cluttered environment containing moving and/or simultaneously deforming obstacle and even dynamic target. For this purpose, after every short time intervals the potential filed needs to be updated while the obstacle(s) and/or target are supposedly kept immobile. The WMR is let to advance a short distance along the admissible newly generated desired trajectory to reach the new position, which is taken as the new starting point for next step. The algorithm is continued until WMR meets the target.

4. Path Tracking Controller Design

The path-tracking problem for nonholonomic mobile robots is formulated here by defining the reference path:

$$\dot{\mathbf{q}}_r = \mathbf{S}(\theta_r)\mathbf{v}_\mathbf{r} \tag{15}$$

In which $\mathbf{S}(.)$ is the Jacobian matrix in relationship (2), $\mathbf{q}_r(t) = \left[x_r(t), y_r(t), \theta_r(t)\right]^T$ is the expected position and orientation of the vehicle as a function of time, and $\mathbf{v}_r(t) = [v_r(t), \omega_r(t)]^T$ is comprised of the linear and the angular speed of the WMR. The reference path is obtained using artificial potential field algorithm.

A suitable speed controller $\mathbf{v}_c(t) = f_c(\mathbf{e}_p, \mathbf{v}_r, \mathbf{K})$ must be found such that $\lim_{t\to\infty}(\mathbf{q}_r - \mathbf{q}) = \mathbf{0}$. Here, $\mathbf{e}_p = [e_1, e_2, e_3]^T$ and $\mathbf{K} = [k_1, k_2, k_3]^T$ represent tracking error and gains of the controller, respectively. Then, the controller input must be defined in such a way that $\mathbf{v}$ approaches $\mathbf{v}_c$ when $t \to \infty$.

The control rule based on back stepping method presented in [21] is adopted for stabilizing the kinematic part given by equation (2) as follows:

$$\mathbf{v}_c = \begin{bmatrix} v_r\cos e_3 + k_1 e_1 \\ \omega_r + k_2 v_r e_2 + k_3 v_r \sin e_3 \end{bmatrix} \tag{16}$$

This relationship is called the back stepping kinematic control (BKC) rule, and k_i's are assumed to positive. $v_r(>0)$ Is the reference linear speed, $\mathbf{e}_P$ is measured in the moving frame and is defined as follows:

$$\begin{aligned} \mathbf{e}_\mathrm{p} &= \begin{bmatrix} e_1 \\ e_2 \\ e_3 \end{bmatrix} \\ &= \begin{bmatrix} \cos\theta & \sin\theta & 0 \\ -\sin\theta & \cos\theta & 0 \\ 0 & 0 & 1 \end{bmatrix}\begin{bmatrix} x_r - x \\ y_r - y \\ \theta_r - \theta \end{bmatrix} \end{aligned} \tag{17}$$

Now, the rate of position error is calculated as follows:

$$\dot{\mathbf{e}}_p = \begin{bmatrix} v_2 e_2 - v_1 + v_r \cos e_3 \\ -v_2 e_1 + v_r \sin e_3 \\ \omega_r - v_2 \end{bmatrix} \tag{18}$$

In addition, the velocity error can be defined by:

$$\mathbf{e}_c = \mathbf{v} - \mathbf{v_c} = \begin{bmatrix} v - v_r \cos e_3 - k_1 e_1 \\ \omega - \omega_r - k_2 v_r e_2 - k_3 v_r \sin e_3 \end{bmatrix} \tag{19}$$

4.1. Integral Sliding Mode Control Design

In this section, the robot kinematic tracking control design using integral sliding mode, which lets the actual velocities of WMR converge to the control velocities generated by the kinematic controller, is explained. Since the dynamic model of the WMR is a first order nonlinear function, the sliding surface with integral term is considered as:

$$\mathbf{s}(t) = \begin{bmatrix} s_1(t) \\ s_2(t) \end{bmatrix} = \mathbf{e_c}(t) + \mathbf{\Lambda} \int_0^t \mathbf{e_c}(\tau)\, d\tau \tag{20}$$

Where $\mathbf{\Lambda} = 0$ is the sliding-surface integral parameter? It is noted in (20) that once the system is on the sliding surface $\mathbf{s} = 0$, then the tracking error $\mathbf{e_c}(\infty) \to 0$ as $\mathbf{\Lambda} > 0$. Hence it is desired to draw the closed-loop system toward the sliding surface $\mathbf{s} = 0$.

Taking time derivative of (20) yields:

$$\dot{\mathbf{s}}(t) = \dot{\mathbf{e}}_\mathbf{c}(t) + \mathbf{\Lambda}.\mathbf{e_c}(t) \tag{21}$$

Neglecting all uncertainties and disturbances and substituting the relations resulted from $\mathbf{s} = \dot{\mathbf{s}} = 0$ condition into the dynamic model; the equivalent control law $\boldsymbol{\tau}_{eq}$ is obtained as:

$$\boldsymbol{\tau}_{eq} = \hat{\mathbf{M}}\dot{\mathbf{s}}_\mathbf{r} + \hat{\mathbf{V}}\mathbf{s_r} \tag{22}$$

In which matrices $\hat{\mathbf{M}}$ and $\hat{\mathbf{V}}$ are nominal mass and nonlinearity matrices, respectively. $\mathbf{s_r}$ And its derivative are defined as:

$$\mathbf{s_r}(t) = \mathbf{v}(t) - \mathbf{s}(t) = \mathbf{v_c}(t) - \Lambda \int_0^t \mathbf{e_c}(\tau) d\tau \tag{23}$$

$$\dot{\mathbf{s}}_\mathbf{r}(t) = \dot{\mathbf{v}}(t) - \dot{\mathbf{s}}(t) = \dot{\mathbf{v}}_\mathbf{c}(t) - \mathbf{\Lambda}.\mathbf{e_c}(t)$$

The equivalent control law $\boldsymbol{\tau}_{eq}$ can make the state of the system to remain on the sliding surface, assuming that process parameters are exactly known. However, to overcome the effects of the uncertainties in the real application, compensation of the equivalent control law using discontinuous control part $\boldsymbol{\tau}_{sw}$ is essential. Thus employing the total control law comprising the summation of equivalent and switching control parts $\boldsymbol{\tau}_{eq}$ and $\boldsymbol{\tau}_{sw}$, in eq. 22, it yields [12].

$$\boldsymbol{\tau} = \boldsymbol{\tau}_{eq} + \boldsymbol{\tau}_{sw} = \hat{\mathbf{M}}\dot{\mathbf{s}}_\mathbf{r} + \hat{\mathbf{V}}\mathbf{s_r} - \mathbf{W}\mathrm{sgn}(\mathbf{s}) \tag{24}$$

Here, $\mathrm{sgn}(\cdot)$ is the sign function, and $\mathbf{W}$ is a diagonal gain matrix by diagonal elements w_i fulfilling the condition of:

$$w_i \geq \left|\tilde{\mathbf{M}}\dot{\mathbf{s}}_\mathbf{r} + \tilde{\mathbf{V}}\mathbf{s_r}\right|_\mathrm{i} + \eta_\mathrm{i} \tag{25}$$

in which η_i's are arbitrary positive constants, $\tilde{\mathbf{M}} = \hat{\mathbf{M}} - \bar{\mathbf{M}}$ and $\tilde{\mathbf{V}} = \hat{\mathbf{V}} - \mathbf{V}$.

The control law (24) along with the conditions (25) guarantees the stability of the controlled plant [12].

In order to reduce the chattering phenomenon, the most common method is to utilize the saturation function $\mathrm{sat}(\mathbf{s}, \phi)$. Thus, replacing $\mathrm{sgn}(\mathbf{s})$ by $\mathrm{sat}(\mathbf{s}, \phi)$ in (24) implies

$$\boldsymbol{\tau} = \boldsymbol{\tau}_{eq} + \boldsymbol{\tau}_{sw} = \hat{\mathbf{M}}\dot{\mathbf{s}}_\mathbf{r} + \hat{\mathbf{V}}\mathbf{s_r} - \mathbf{K}\mathrm{sat}(\mathbf{s}, \phi) \tag{26}$$

Where

$$\mathrm{sat}(\mathbf{s}_\mathrm{i}, \phi_\mathrm{i}) = \begin{cases} \mathrm{sign}(\mathbf{s}_\mathrm{i}) & \text{if } \left|\mathbf{s}_\mathrm{i} / \phi_\mathrm{i}\right| > 1 \\ \mathbf{s}_\mathrm{i} / \phi_\mathrm{i} & \text{if } \left|\mathbf{s}_\mathrm{i} / \phi_\mathrm{i}\right| \leq 1 \end{cases}, \quad \mathrm{i}=1,2 \tag{27}$$

And ϕ_i (i=1,2) is a small positive constant.

4.2. Adaptive Integral Sliding Mode Control Design

In this section, the regress or based adaptive integral sliding control method proposed in [27] has been used for mobile robot dynamics. Regression models investigate relationship between variables in a system and they are based on the observations of the independent and dependent variables. The function is to predict the

dependent variable is built. In fact, by using of this relation the uncertainty transforms from the state to parameters.

Using the linearity property of the robot dynamics than the uncertainty parameters, robot dynamic regression model can be expressed as follows:

$$\begin{Bmatrix}\tau_1\\ \tau_2\end{Bmatrix}=\begin{bmatrix}\dot{v} & -v\omega & 0\\ 0 & \omega^2 & \dot{\omega}\end{bmatrix}\begin{Bmatrix}m\\ md\\ I_G+md^2\end{Bmatrix} \quad (28)$$
$$=\mathbf{Y(v)\alpha}$$

Where $\boldsymbol{\alpha}$ is an uncertainty parameters vector that must be estimated and $\mathbf{Y(v)}$ is known as a regressor (certain part) of the mobile robot? Here, such as the equivalent part of the control law in the previous subsection can be defined the regressor matrix for the without disruption and uncertainty state of the nominal model (22) as:

$$\hat{\mathbf{M}}\dot{\mathbf{s}}_r+\hat{\mathbf{C}}(\mathbf{v})\mathbf{s}_r=\mathbf{Y}_1(\mathbf{v},\mathbf{s}_r,\dot{\mathbf{s}}_r)\hat{\boldsymbol{\alpha}} \quad (29)$$

Where $\hat{\boldsymbol{\alpha}}$ is estimate of the uncertainty parameters vector $\boldsymbol{\alpha}$ and $\mathbf{Y}_1(\mathbf{v},\mathbf{s}_r,\dot{\mathbf{s}}_r)$ is defined as:

$$\mathbf{Y}_1(\mathbf{v},\mathbf{s}_r,\dot{\mathbf{s}}_r)=\begin{bmatrix}\dot{s}_{r_1} & -s_{r_2} & 0\\ 0 & s_{r_2} & \dot{s}_{r_2}\end{bmatrix} \quad (30)$$

Thus, control law with used the above equation is chose as the following form:

$$\boldsymbol{\tau}=\mathbf{Y}_1(\mathbf{v},\mathbf{s}_r,\dot{\mathbf{s}}_r)\hat{\boldsymbol{\alpha}}-\mathbf{K}_1\mathbf{s} \quad (31)$$

Where includes a "feed forward" term $\mathbf{Y}_1(\mathbf{v},\mathbf{s}_r,\dot{\mathbf{s}}_r)\hat{\boldsymbol{\alpha}}$ which is the same as the term $\boldsymbol{\tau}_{eq}$ of the robust integral sliding mode controller, in addition to a simple PI term $\mathbf{K}_1\mathbf{s}$. Lyapunov stability is used to achieve adaptive control law to estimate the $\hat{\boldsymbol{\alpha}}$ as follow:

$$\dot{\hat{\boldsymbol{\alpha}}}=-\boldsymbol{\Gamma}\mathbf{Y}_1^{\mathrm{T}}\mathbf{s} \quad (32)$$

Where $\boldsymbol{\Gamma}$ is a diagonal matrix with arbitrary positive elements?

The final structures of hybrid real-time harmonic potential field with BKC+ISMDC and BKC+AISMDC path tracking control system of three – wheel nonholonomic mobile robots are shown in Figs. 3 and 4, respectively.

These diagrams are each comprise of three blocks: Harmonic potential field, Backstepping kinematic controller, and Integral/adaptive integral sliding mode dynamic controller. The first block provides the reference path and orientation information to be followed by the WMR. In the second block, the kinematic controlling strategy is implemented. The outcome of this block which is the kinematically controlled speed is fed as the reference input to the last block. In this last block, based on the integral/adaptive integral sliding mode control method, the control effort is calculated and is fed to the robot dynamic model. The calculated speed is transformed to generalized coordinates, and then is integrated to give the robot's position and orientation.

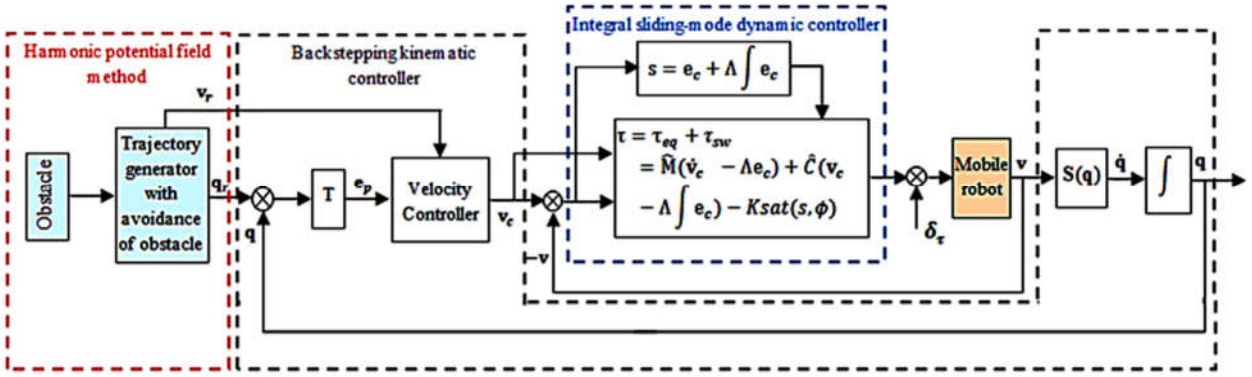

Fig. 3. The structure of the BKC+ISMDC algorithm.

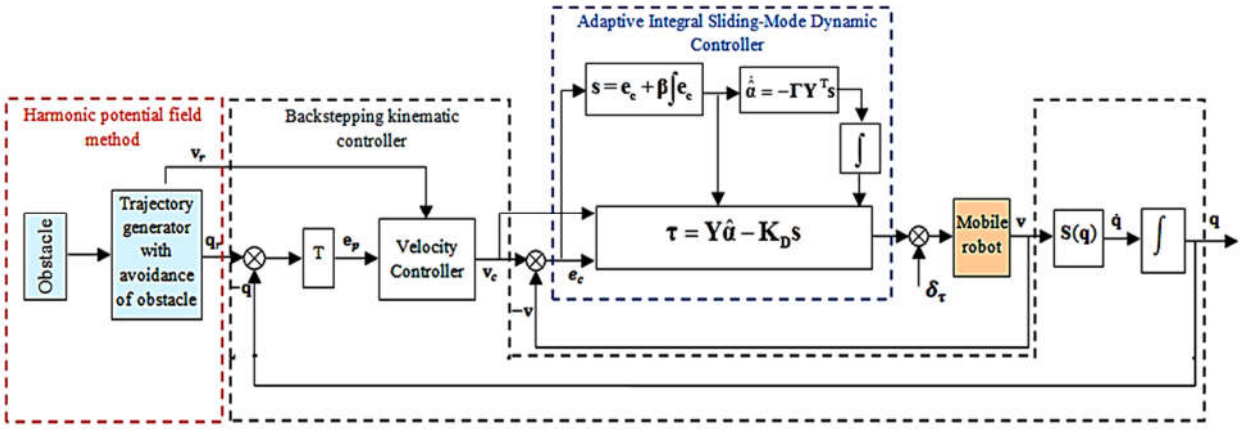

Fig. 4. The structure of the BKC+AISMDC algorithm.

5. Results and discussion

To investigate the performance of the reference path generating algorithm along with the proposed combined kinematic and dynamic trajectory tracking controllers, a proper simulation program is developed, which is sufficiently flexible to examine the integrated algorithm for various shapes of the obstacles. It also allows to investigate the robot's reaction in case of confronting an unstructured variable size moving obstacle.

A case study is conducted to examine the performance of the robot using each control method along with the real time harmonic potential path-planning algorithm, while the robot confronts a variable-size triangular shape dynamic obstacle, and is simultaneously exposed to wheel torque disturbances and plant uncertainties. Robot's nominal parameters as well as their uncertainties are listed in Table 1.

Table. 1. Parameters of the dynamic model of WMR including nominal and real values as well as assumed uncertainties.

Parameter	Nominal Parameters	Real Parameters			%Uncertainty
		t < 2	2 < t < 4	t > 4	
m(kg)	5	5	6	10	25%
I_G (kg.m^2)	2.5	2.5	3.5	6	50%
d(m)	0.1	0.1	0.12	0.15	25%
r(m)	0.03	0.03	0.03	0.03	0%
L(m)	0.15	0.15	0.15	0.15	0%

All of the assumed gains of the controllers and related parameters for the control algorithms are given in Table 2. In the simulations, the symbol ⌦ is used to represent the robot, in which its tip shows the orientation of the robot along the path.

Table. 2. Gains of the controllers and the parameters used for path planning algorithm.

BKC	ISMDC	AISMDC	Path generator	
$k_1 = 20$	$\eta_1 = \eta_2 = 10$	$\mathbf{K_D} = \begin{bmatrix} 500 & 0 \\ 0 & 400 \end{bmatrix}$	$\lambda_g = 30$	Starting point (-1,-4)
$k_2 = 10$	$\mathbf{\Lambda} = \begin{bmatrix} 100 & 0 \\ 0 & 150 \end{bmatrix}$	$\boldsymbol{\beta} = \begin{bmatrix} 200 & 0 \\ 0 & 300 \end{bmatrix}$	$U = 1$	Goal point (1,3)
$k_3 = 3$	$\phi_1 = \phi_2 = 0.01$	$\mathbf{\Gamma} = \begin{bmatrix} 1 & 0 & 0 \\ 0 & 1 & 0 \\ 0 & 0 & 1 \end{bmatrix}$	$\alpha = 1.292$	Select the safest path

The desired linear velocity along the path is assumed to be:

$$v_r = \begin{cases} 2.8\left|\mathbf{x}-\mathbf{P_s}\right|+0.1 & \text{if } \left|\mathbf{x}-\mathbf{P_s}\right| < 0.5 \\ 1.5\left|\mathbf{x}-\mathbf{P_g}\right| & \text{if } \left|\mathbf{x}-\mathbf{P_g}\right| < 1 \\ 1.5 & \text{otherwise} \end{cases} \quad (33)$$

Where $\mathbf{x}$, $\mathbf{P}_s$ and $\mathbf{P}_g$ are coordinates of robot's current position (point P if Fig. 1), starting point, and goal point, respectively. This corresponds to a second order polynomial smooth acceleration in start; followed by a constant speed regime, and then a second order polynomial

smooth deceleration before stop. The robot comes to rest in target. The amplitude of the input torques are limited to 15 N.m to accommodate the results as much as possible with the actual conditions.

As mentioned in Section 3, the algorithm could be employed for real time applications. It is assumed that after every short time intervals the potential filed is updated while the obstacle and/or target are supposedly kept immobile. The safe route with the attribute of desired level of collision avoidance control of the robot with the obstacles is continuously established using condition (12). In order to present the robustness of the control methods eliminating the effects of the disturbances, the robot is proposed to be imposed to the external disturbances plotted in (5).

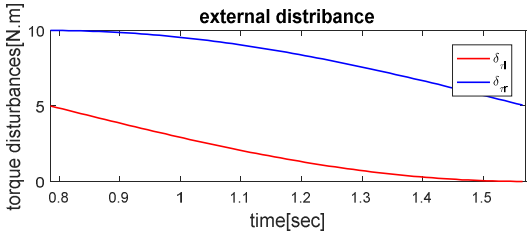

Fig. 5. external disturbance in torque of the wheels

The results of the simulation program for an equilateral triangular obstacle are presented in Figs. 6 to 11 imposed to the external disturbances. The obstacle is assumed a sized changed moving triangle on a circular path around the goal, change of the sides.

The complete process of the robot trajectory in the presence of resizable moving triangular obstacle is plotted in Fig. 6, showing robot's reaction confronting the moving obstacle in one picture.

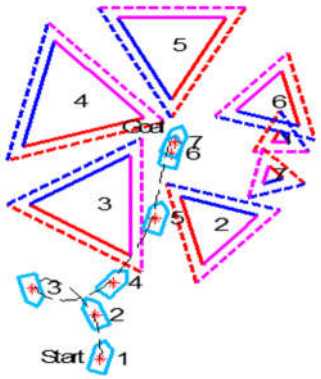

Fig. 6. the corresponding complete process of the robot trajectory

The power per unit length of the panels as a function of time is plotted in Fig. 7. Acting the panels as a source or sink and variation of their power per unit length are directly related to the instant position of the panels than the robot. Closeness of robot and obstacle remarkably affects the produced powers of the panels, in which the closest panel to robot shows the highest power.

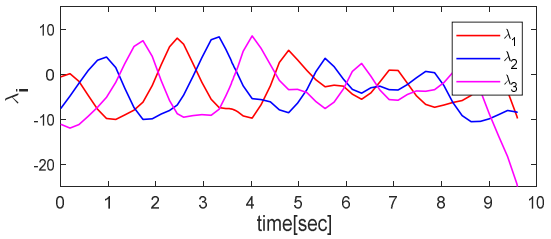

Fig. 7. Power per unit length of each panel for variable-size equilateral triangular obstacle.

The Power of the panel facing the robot reaches its highest level at the closest distance and then gradually changes due to receding from the robot and reduction in the size of the obstacle. The ability of adjusting the power of the panels is the key issue of the proposed algorithm, which guarantees the robot and obstacle collision avoidance while maintaining a smooth movement.

The corresponding complete trajectory tracking process of the robot are plotted in Figs. 8a-8f different successive times with $\pi/2$ sec time intervals. The figures showing the fact that the resulted harmonic potential pattern in the presence of the dynamic obstacle as the robot moves toward the goal.

These figures quite descriptively show the flow pattern around the obstacle and the direction of the flow field oriented toward the goal (sink), which is indeed in compliance with the theory.

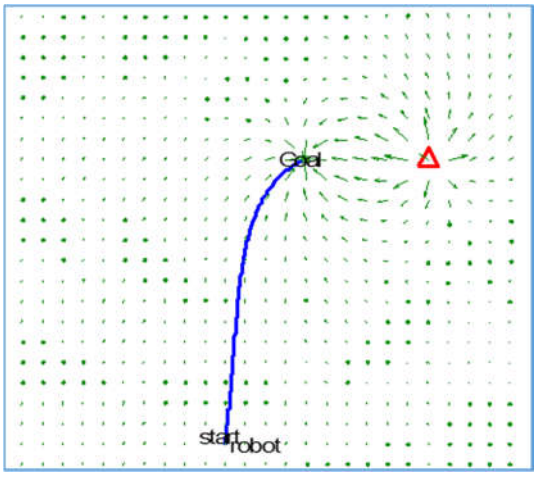

(a) at t = 0 sec

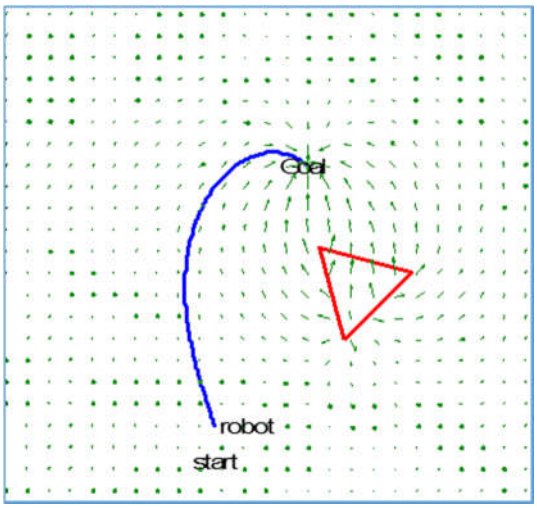

(b) at t = π/2 sec

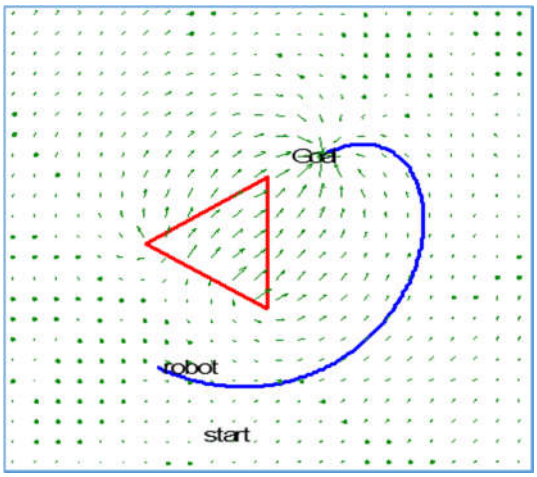

(c) at t = π sec

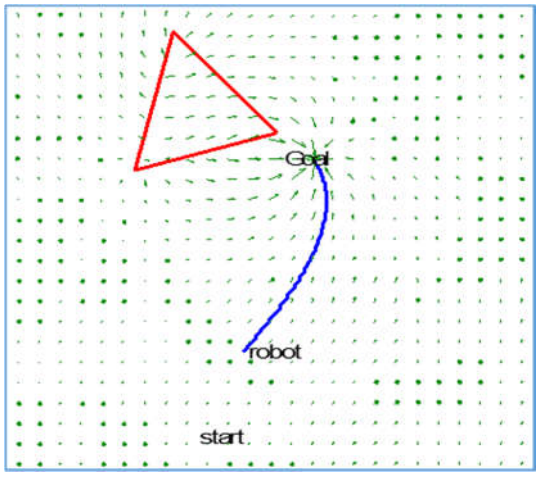

(d) at t = 3π/2 sec

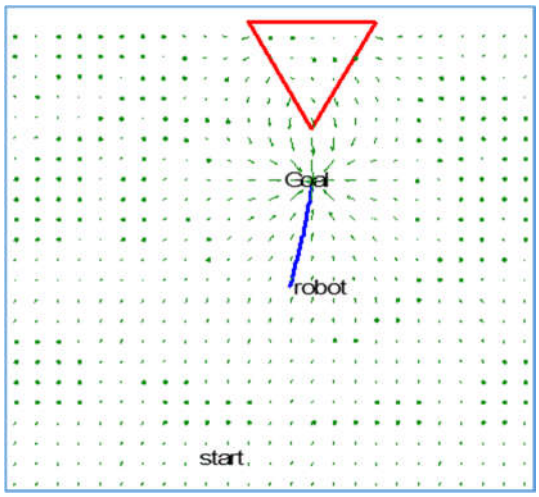

(e) at t = 2π sec

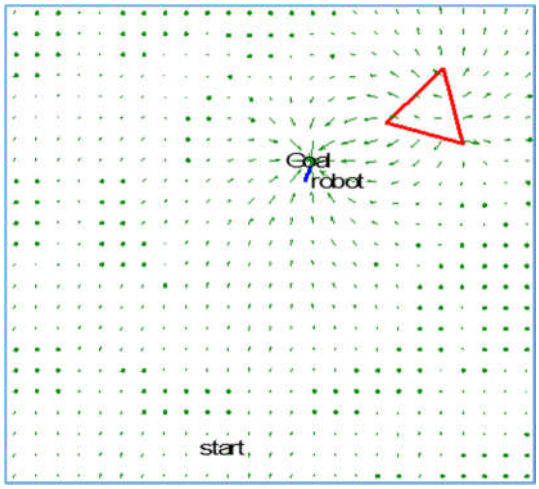

(f) at t = 5π/2 sec

Fig. 8. The corresponding complete trajectory tracking process of the robot at different successive time intervals.

In addition to the changes of the potential field, the corresponding routes at each instances are also depicted to show the capability of the path-planning algorithm to adapt with the field condition. As it is seen, the robot trajectory and orientation is designed such that it is safely kept away from obstacle, while the obstacle approaches toward it. The reference trajectory in this case is planned such that the robot carries out a complete turn to bypass the obstacle and then moves toward the goal along the reference path.

The same practice is examined while taking the size uncertainty of the obstacle into consideration. The results of this study are plotted in Figs. 9a and 9b. These figures reveal the effectiveness of the employed control methods of dynamic uncertain obstacle collision avoidance. The robot's position and orientation in the most prominent critical condition facing the obstacle is shown by no. 3.

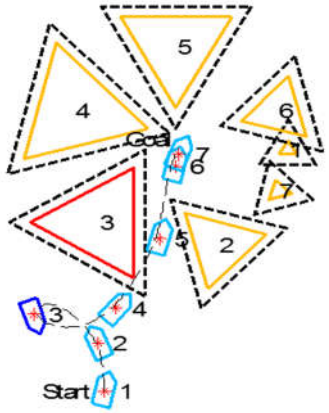

(a)

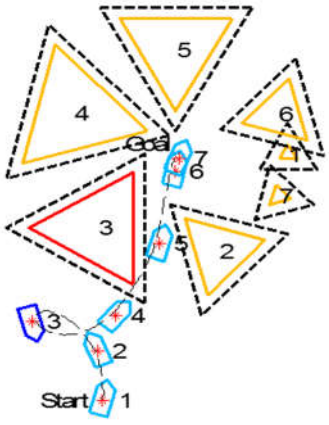

(b)

Fig. 9. Tracking of the generated path in the presence of a variable-size triangular regularly shape dynamic obstacle with used a (a) BKC+ISMDC, (b) BKC+AISMDC

The performance of path tracking controllers under parameter variations and input disturbances are depicted in figures 10. Figures 10a and 10b show the quality of the BKC+ISMDC control algorithm in following the reference linear and angular velocities, respectively. The same graphs for the BKC+AISMDC algorithm are plotted in figures 9c and 9d. It is clear that the control objective in rejecting the effects of the disturbances is almost achieved using BKC+AISMDC control method.

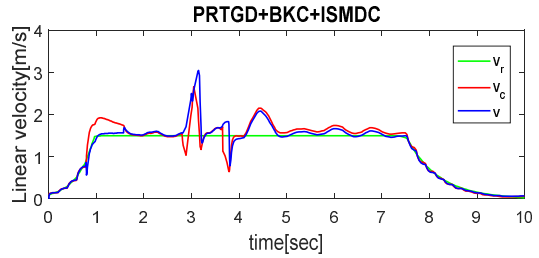

(a)

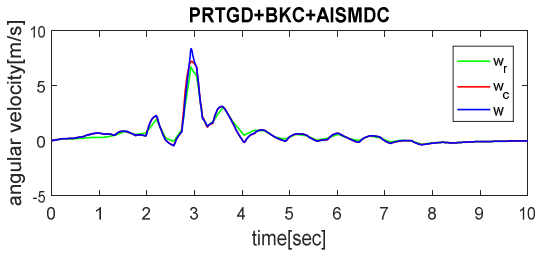

(b)

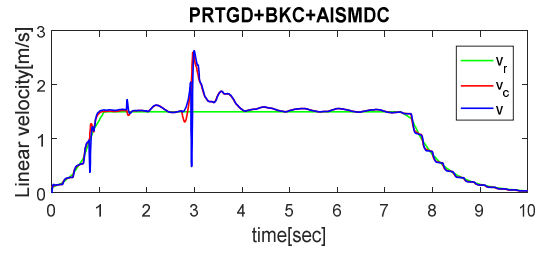

(c)

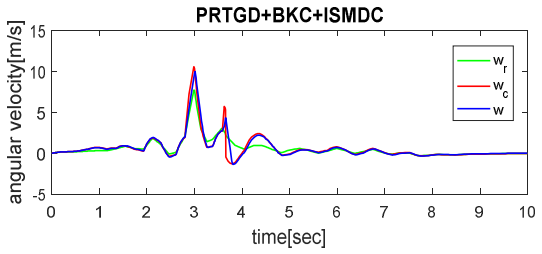

(d)

Fig. 10. The comparisons of the tracking control ability of the BKC+ISMDC and the BKC+AISMDC under parameter variations and disturbances. (a) And (b) The linear speed tracking errors. (c) And (d) The angular speed errors.

The controlled torques for both controllers are illustrated in figures 11a to 11b, respectively. The highest limit of the input torques are bounded below 15 N.m.

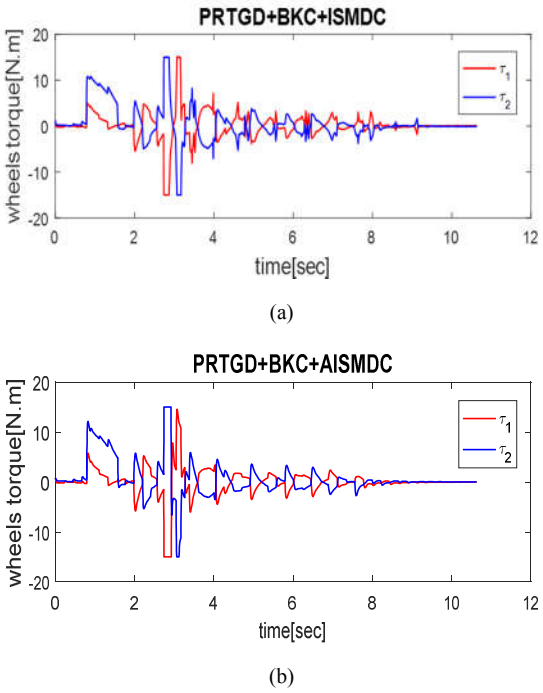

Fig. 11. Torque generated for the rear wheels of the robot with used a (a) BKC+ISMDC, (b) BKC+AISMDC

As shown, BKC+AISMDC method consumes rather less a smoother control effort compared to its counterpart, although it poses slightly better performance in fulfilling the overall control objectives.

The performance index of square errors of the control method is used to further illustrate the quality of the both hybrid control methods. Since each algorithm employs two cascade controllers for kinematics and dynamic parts, two sets of comparative figures are generated. The ISE index for the task space variables as the linear and angular speed errors in Figs. 12a and 12b. In each case BKC+AISMDC shows better performance against BKC+ISMDC. The same index for the so-called joint variable errors (e1, e2 and e3) are plotted in Figs. 12c and 12d. In each case BKC+AISMDC shows better performance against BKC+ISMDC. Investigating the results reveals better performance of the BKC+AISMDC algorithm against its counterparts.

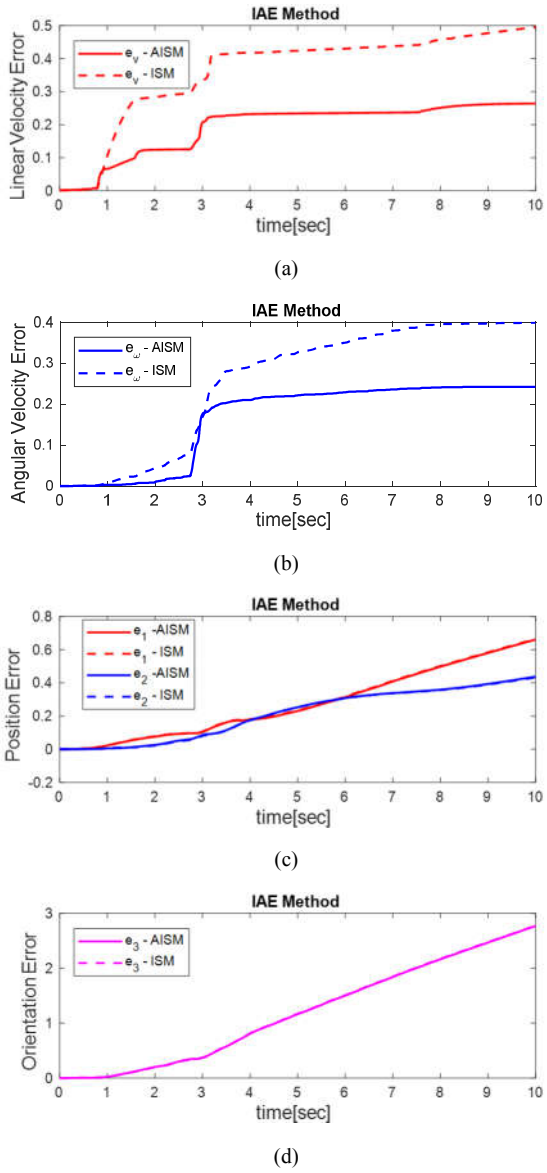

Fig. 12. Integral of square error performance index (a) linear velocity, (b) angular velocity, (c) absolute positions, and (d) orientation erros.

6. Conclusion

In this article, the effectiveness of the real-time harmonic potential path planning algorithm based on the panel method along with the hybrid backstepping kinematic and adaptive integral sliding mode dynamic trajectory tracking control of the three-wheel nonholonomic mobile robot in presence of the variable-size dynamic obstacle has been investigated. To further clear up the outperformance of the adaptive dynamic controller part, its performance is compared with the conventional integral sliding mode

dynamic controller. In all cases the investigation is carried out for the robot with model uncertainties and susceptible to wheels torque disturbances. Results of the conducted simulations reveals the capability of the proposed robust collision avoidance real-time path planning method along with the hybrid kinematic and dynamic control algorithms as an effective control solution of the wheeled mobile robots to safely perform in the dynamic clutter environment imposed to the disturbances and model uncertainties.

References

[1] Ashoorirad, M.; Barzamini, R.; Afshar, A.; Jouzdani, J., "Model reference adaptive path following for wheeled mobile robots" in Information and Automation, 2006. ICIA 2006. International Conference on. 2006. IEEE (2006).

[2] Nawash, N., "H-infinity Control of an Autonomous Mobile Robot" 2005, Cleveland State University (2005).

[3] Siegwart, R.; Nourbakhsh, I.R.; Scaramuzza, D., "Introduction to autonomous mobile robots": MIT press (2011).

[4] Daily, R.; Bevly, D.M., "Harmonic potential field path planning for high speed vehicles. in American Control Conference", 2008. IEEE (2008).

[5] Klancar, G.; Matko, D.; Blazic, S., "Mobile robot control on a reference path in Intelligent Control', 2005. Proceedings of the 2005 IEEE International Symposium on, Mediterrean Conference on Control and Automation. IEEE (2005).

[6] Lepetič, M.; Klančar, G.; Škrjanc, I.; Matko, D.; Potočnik, B., "Path planning and path tracking for nonholonomic robots" Mobile robots: new research. New York: Nova Science, cop, pp. 341-364 (2005).

[7] Khatib, O., "Real-time obstacle avoidance for manipulators and mobile robots". The international journal of robotics research, 5(1), pp. 90-98 (1986).

[8] Kim, J.; Khosla, P., "Real-time obstacle avoidance using harmonic potential functions" in Robotics and Automation, 1991. Proceedings, 1991 IEEE International Conference on. (1991).

[9] Ferrara, A.; Rubagotti, M., "Second-order sliding-mode control of a mobile robot based on a harmonic potential field". IET Control Theory & Applications, 2 (9), pp. 807-818 (2008).

[10] Fahimi, F.; Ashrafiuon, H.; Nataraj, C., "Obstacle Avoidance for Spatial Hyper-Redundant Manipulators Using Harmonic Potential Functions and the Mode Shape Technique". Journal of Robotic Systems, 20(1), pp. 23-33 (2003).

[11] Fahimi, F.; Ashrafiuon, H.; Nataraj, C., "Obstacle Avoidance for Groups of Mobile Robots Using Potential Field Technique". in ASME 2004 International Mechanical Engineering Congress and Exposition. American Society of Mechanical Engineers (2004).

[12] Fahimi, F., "Autonomous robots: modeling, path planning, and control". Springer Vol. 107. (2008).

[13] Fahimi, F.; Ashrafiuon, H.; Nataraj, C., "Real-time obstacle avoidance for multiple mobile robots". Robotica, 27(2). pp. 189-198 (2009).

[14] Huang, L., "Velocity planning for a mobile robot to track a moving target – a potential field approach". Robotics and Autonomous Systems, 57(1). pp. 55-63 (2009).

[15] Szulczyński, P.; Pazderski, D.; Kozłowski, K., "Real-time obstacle avoidance using harmonic potential functions". Journal of Automation Mobile Robotics and Intelligent Systems,vol. (5) pp. 59-66 (2011).

[16] Heidari, M.; Nikranjbar, A.; Ataei, A.A., "Trajectory Tracking Kinematic Control of the Mobile Nonholonomic Robot using Backstepping Approach", in Int. Conf. Mechanical Engineering and Advanced Technology (ICMEAT). Isfahan, Iran (2012).

[17] Heidari, M.; Nikranjbar, A.; Ataei, A.A., "Integral Sliding Mode Trajectory Tracking Control of Nonholonomic Mobile Robots Based on the Harmonic Potential Field Approach", in 11th Intelligent Systems Conference. Intelligent systems scientific society of Iran: Tehran, Iran (2013).

[18] Masoud, M.; Nikranjbar, A.; Ataei, A.A., "A harmonic potential field approach for joint planning and control of a rigid, separable nonholonomic, mobile robot". Robotics and Autonomous Systems. 61(6), pp. 593-615 (2013).

[19] Panati, S.; Baasandorj, B.; Chong, K.T., "Autonomous Mobile Robot Navigation Using Harmonic Potential Field", in IOP Conference Series: Materials Science and Engineering. IOP Publishing (2015).

[20] Yang, J.M.; Kim, J.H., "Sliding mode control for trajectory tracking of nonholonomic wheeled mobile robots". Robotics and Automation, IEEE Transactions on, 15(3), pp. 578-587 (1999).

[21] Fierro, R.; Lewis, F.L., "Control of a nonholonomic mobile robot: backstepping kinematics into dynamics", in Decision and Control, Proceedings of the 34th IEEE Conference on. 1995. IEEE (1995).

[22] Chen, C.Y.; Li, T.H.S.; Yeh, Y.C.; Chang, C.C., "Design and implementation of an adaptive sliding-mode dynamic controller for wheeled mobile robots". Mechatronics, 19(2), pp. 156-166 (2009).

[23] Wu, Y.; Hu, Y., "Kinematics, dynamics and motion planning of wheeled mobile manipulators". Pro of Int on CSIMTA, 2004. 4: pp. 221-226 (2004).

[24] Solea, R.; Filipescu, A.; Nunes, U., "Sliding-mode control for trajectory tracking of a wheeled mobile robot in presence of uncertainties", in Proceedings of the 7th Asian Control Conference. (2009).

[25] Kokotovie, P.V., "The joy of feedback: nonlinear and adaptive". IEEE Control Systems Magazine, 1992. 12(3), pp. 7-17 (1992).

[26] Marquez, H.J., "Nonlinear control systems: analysis and design". John Wiley (2003).

[27] Slotine, J.J.E.; Li, W., "Applied nonlinear control". Prentice-Hall Englewood Cliffs, NJ. Vol. 199 (1991).

[28] Mehrjerdi, H.; Saad, M., "Dynamic tracking control of mobile robot using exponential sliding mode", in IECON 2010-36th Annual Conference on IEEE Industrial Electronics Society. IEEE (2010).

[29] Keighobadi, J.; Mohamadi, Y., "Fuzzy Sliding Mode Control of non-holonomic Wheeled Mobile Robot", in Applied Machine Intelligence and Informatics (SAMI), 2011 IEEE 9th International Symposium on. IEEE (2011).

[30] Wu, J.; Xu, G.; Yin, Z., "Robust adaptive control for a nonholonomic mobile robot with unknown parameters". Journal of Control Theory and Applications, 7(2), pp. 212-218 (2009).

[31] Wang, Y.T.; Chen, Y.C.; Lin, M.C., "Dynamic Object Tracking Control for a Non-Holonomic Wheeled Autonomous Robot". Tamkang Journal of Science and Egineering, 12(3), pp. 339-350 (2009).

[32] Kim, J.O.; Khosla, P.K., "Real-time obstacle avoidance using harmonic potential functions". Robotics and Automation, IEEE Transactions on, 8(3), pp. 338-349 (1992).